



Structural Health Monitoring in Aerospace: Integrating Sensor Technologies for Enhanced Safety and Efficiency

Vaishnavi Negi¹, Mansha Arora¹, Samarth Khanadale¹, Honey Kumari¹, and Vishnu Vijay Kumar^{2,*}

¹ International Institute of Aerospace Engineering and Management,

Jain deemed-to-be-University, JGI global campus, Bangalore- 562112, India

² Structural Engineering, Division of Engineering, New York University Abu Dhabi (NYUAD), 129188 Abu Dhabi, United Arab Emirates

Corresponding author's email: vishnu.vijaya@u.nus.edu

Abstract. Ensuring structural integrity in aircraft is vital for safe operation. This study explores the application of Structural Health Monitoring (SHM) systems in aviation, focusing on advanced sensor technologies and data processing techniques. We instrumented a representative aircraft component with strain gauges, accelerometers, and acoustic emission sensors to monitor critical structural loads and damage initiation. The key finding is the validation of SHM's capability to enhance safety, reduce maintenance costs, and extend aircraft service life by providing real-time data on structural health. This work emphasizes SHM as essential for modern aircraft maintenance and safety management. This study offers a comprehensive overview of SHM applications in aviation, aiming to elucidate its role, examine various sensor technologies, explore data processing techniques, and showcase practical implementations. We investigate how SHM enhances safety, reduces maintenance costs, and extends aircraft service life. Our research employed a holistic approach encompassing data acquisition, analysis methodologies, and algorithm development. The sensors were strategically positioned to capture data on critical structural loads, vibrations, and damage initiation and progression.

Keywords: Structural Health Monitoring, Aerospace, Reliability, Composite, Sensors.

1 INTRODUCTION

SHM has emerged as a critical technology in aerospace, civil, and mechanical engineering, offering a systematic approach to analyse, identify, and document the loading and damage conditions of structures via integrated sensing devices[1], [2], [3], [4]. Zhang et al. [5]noted that SHM represents a paradigm shift in damage detection strategies, particularly in the aviation industry, where safety and operational efficiency are paramount. The evolution of SHM systems has been marked by significant advancements in sensor technologies and data processing techniques. Recent studies highlight the integration of vibration monitoring, which has long been used in rotating machinery, into more complex structures such as aircraft wings and building infrastructures[6]. This integration allows for a comprehensive understanding of the load– structure–response chain, which is crucial for design validation and performance

© The Author(s) 2025

M. A. Muflikhun et al. (eds.), *Proceedings of the 10th International Conference on Science and Technology (ICST 2024)*, Advances in Engineering Research 268,

https://doi.org/10.2991/978-94-6463-772-4_23

optimization. The key components of modern SHM systems include damage detection, localization, assessment, prognosis and recommendation of corrective actions, validation of novel design parameters, early detection of potential deterioration, monitoring of abnormal loading and responses, real-time safety evaluation of post-extreme events, prioritization of maintenance and repair activities, evaluation of new structural types and smart material applications[7], [8], [9]. Chen et al. [10] emphasized the importance of beam structures as fundamental components in construction and engineering. Their research demonstrated that SHM approaches for beam analysis can be divided into two main categories: wave propagation and vibration-based techniques. These methods enable a deeper understanding of structural behaviours under various loads and environmental conditions. A typical SHM system, consists of a diagnostic component for damage detection and assessment and a prognostic component for evaluating the implications of detected damage. The selection of sensor types, numbers, and positions, along with data acquisition and transmission systems, forms the hardware backbone of SHM, often referred to as health and usage monitoring systems. Data normalization plays a crucial role in SHM. This process involves distinguishing between sensor reading changes caused by damage and those resulting from environmental and operational factors. Normalization techniques may involve comparing measured responses to inputs or temporally aligning data to account for operational cycles. To fully leverage the potential of SHM, a rigorous design and implementation approach is essential. As noted by Sun et al.,[11] SHM serves as a complementary tool to traditional methods such as visual inspection and finite element modelling (FEM), enhancing overall safety and management strategies in structural engineering[12]. SHM continues to evolve as a critical technology for ensuring the safety, efficiency, and longevity of engineering structures, particularly in the aviation industry. This study demonstrates, the integration of advanced sensor technologies, data processing techniques, and innovative testing methodologies in SHM systems offers a promising path toward enhancing aircraft safety, optimizing maintenance procedures, and extending the operational lifespan of aerospace structures in an increasingly complex and demanding aviation environment. Traditional methods, such as manual inspection and ultrasound techniques, often fail to detect hidden or early-stage damage, which can lead to catastrophic failures. For instance, in the 2014 incident involving an Airbus A380, an engine turbine suffered a failure due to an undetected fatigue crack. This failure resulted in significant damage to the engine and aircraft, highlighting the limitations of conventional inspection methods.

Structural Health Monitoring can address the growing challenge of ensuring aircraft safety and extending operational lifespan while minimizing maintenance costs. The problem lies in the current reliance on periodic inspections, which can fail to detect early-stage damage or operational inefficiencies. This study seeks to prove that integrating advanced SHM technologies can offer a more reliable, real-time solution to these issues. By implementing SHM techniques, such as advanced sensors and real-time monitoring systems, it's possible to detect structural damage at its earliest stages. This proactive approach enables timely maintenance and repairs, ensuring safer operations and reducing the risk of accidents caused by undetected flaws or fatigue cracks.

2 METHODOLOGY

Two plates of 150 X 150 sq. mm each, one made of an acrylic plate and the other made of a carbon glass hybrid fibre composite, were used for testing. Sensors play a crucial role in SHM by providing essential data for understanding the structural integrity of components. Any unexpected shift in sensor output can signal potential failure or the propagation of cracks. The SHM process employing sensors involves continuous data monitoring, subsequent data interpretation, and, ultimately, the storage and analysis of acquired data. Various sensors were deployed to monitor specific physical quantities, such as displacement and vibrations. These measurements offer a clear indication of the structural load the component is experiencing. Based on sensor outputs, we can assess the behaviour of the structure, exemplified here by a cantilever beam, under specific loading conditions. Load cell: The applied force measurement is crucial in SHM to achieve this goal when a load cell is used. A load cell is an instrument that we employ for this purpose. They are a type of transducer that converts an applied force into an electrical signal.



Fig 1. Load cell used in the current experiment

While other types of load cells are available, the most common type is a cell composed of strain gauges from which the electrical signal is obtained via the Wheatstone Bridge instrumentation circuit. The working principle is that as the applied force and resistance increase, the voltage that is produced decreases in value. The load cell used for this experiment is depicted in Figure 1.

Accelerometers are a particular kind of kinematic sensor that is primarily used to analyze an object's motion without considering the reason behind the movement. When a structure is being observed, this device detects oscillatory movement because of induced vibration, which causes changes in acceleration. Every time a metal ball was successfully dropped, the vibration data were examined to determine how it affected the cantilever beam and to track the overall health of the beam. The accelerometer was attached to the national instrument and digital output, which were recorded and analysed, to measure the data, or as we like to call the data acquisition process. The accelerometer was fixed on the fixed end of the beam via an adhesive mounting technique. Figure 2 shows the sensors being mounted on the test plate.

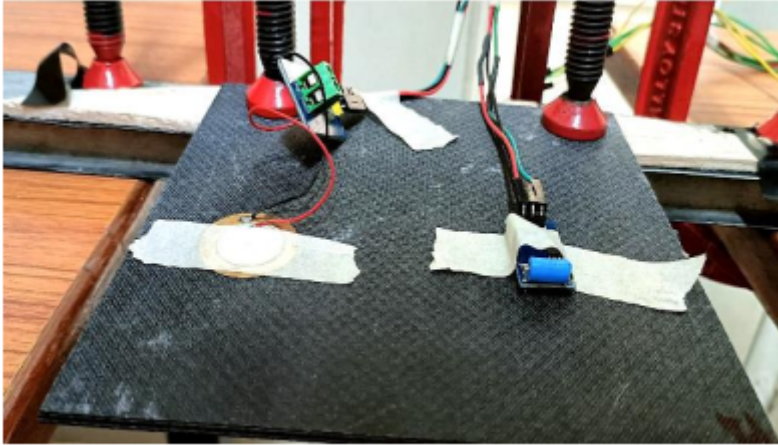


Fig 2. Sensors mounted on a plate

examined to determine how it affected the cantilever beam and to track the overall health of the beam. The accelerometer was attached to the national instrument and digital output, which were recorded and analysed, to measure the data, or as we like to call the data acquisition process. The accelerometer was fixed on the fixed end of the beam via an adhesive mounting technique. Figure 2 shows the sensors being mounted on the test plate.

Table 1. Instrument and Specifications

SI No.	Component	Specification	Function
1.	 <p>National Instrument</p>	<p>USB Bus Powered: Yes (5V via USB)</p> <p>Analog Input (AI):</p> <ul style="list-style-type: none"> • Number of Channels: 8 single-ended or 4 differential channels • Resolution: 14 bits • Input Voltage Range: ± 10 V <p>Analog Output (AO):</p> <ul style="list-style-type: none"> • Number of Channels: 2 • Resolution: 12 bits • Output Voltage Range: ± 10 V • Output Current Drive: ± 2 mA <p>Digital Input/Output (DIO):</p> <ul style="list-style-type: none"> • Number of Channels: 12 (8 DI and 4 DO) • Digital I/O Voltage Levels: TTL (5V logic) • Input Voltage 	<p>The NI USB-6001 is an affordable, multifunction data acquisition (DAQ) device tailored for fundamental tasks such as data logging, measurement, and control</p>

Sl No.	Component	Specification	Function
2.	Arduino Uno 	Threshold: • Low: 0.8 V max • High: 2.2 V min • Drive Strength: ± 3.2 mA[13] • Microcontroller: ATmega328P • Operating Voltage: 5V • Input Voltage (recommended): 7-12V • Input Voltage (limit): 6-20V • Digital I/O Pins: 14 (of which 6 provide PWM output) • Analog Input Pins: 6[14]	It is utilized to gather and process information from sensors that monitor parameters such as structural stress, strain, and vibration.
3.	Capacitance Accelerometer[15] 	• Operating Voltage: 3.3 ~ 5 VDC • Comparator output, clean signal, good waveform, strong driving ability, >15mA • Output format: digital switching output (0 and 1)	These accelerometers offer high accuracy in tracking stress and strain, which are essential factors for assessing the structural soundness of buildings, bridges, and other vital infrastructures.
4.	Piezoelectric Accelerometer 	• Working voltage: 3.3V – 5V DC • Operating current: <1mA • Output: Analog[16]	They can detect high frequency vibrations, which are essential for spotting early indications of structural wear or damage
5.	Load Cell Rees52 	22 cm (8.5 in) wire leads pre attached. Dimensions: 0.5 in x 0.5 in x 3.15 in. 4 mounting holes, 15 mm spacing on each side. One both holes tapped M4 thread, the other side both holes tapped M5 thread.	Load cell was used to obtain the load value at impact

Figure 3 shows the total block diagram of the SHM system being employed during the testing. Piezoelectric vibration sensor: This sensor uses quartz's ability to dissipate charge in response to applied force to measure vibration, acceleration, and

other phenomena. We combined an accelerometer and a piezoelectric vibration sensor to better understand the dynamics of the system. While piezoelectric vibration sensors can measure vibrations and shocks, they may not always provide accurate measurements of linear acceleration, particularly in gravitational fields. Moreover, an accelerometer is used to measure acceleration under the influence of a gravitational field and other forces acting on it.

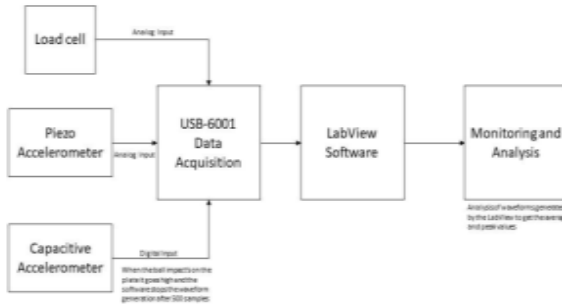


Fig 3. Block Diagram of the SHM system

The piezoelectric sensor can record and analyze the mechanical vibrations and shocks that a system experiences, whereas the accelerometer offers accurate data on linear accelerations. During the test, capacitive and piezoelectric accelerometers were the two kinematic sensors used for measuring the motion caused by an external force. By determining the displacement, velocity, or acceleration of the test structure, this motion can be recorded. Additionally, USB-6001 was used as a data acquisition device in the test. USB-6001 is intended for applications such as simple data logging, portable measurements, and academic laboratory studies. With screw-terminal connectivity, it can quickly connect sensors and signals to USB-6001. The sampling rate was 10 samples per second. Data storage and analysis- To distinguish the data when the ball bearing hit the cantilever beam, the following algorithm was used.

1. A sensor's output data varies when a ball is dropped. To keep track of when this dropping event happens. A variable called "drop event" is set to false, indicating that no drop has occurred yet. A timer is set to 75 μ s (to store the dataset of the variation caused in the output data to understand what is happening after the drop event).
2. Run it in a loop and constantly check if the digital input is true, which will indicate that something has been dropped. The moment it detects a drop (when the input becomes true), it denotes the current time.
3. From the moment it detects the drop (when the input turns true) and, for the next 75 μ s, starts capturing data during this tiny timeframe. This could be done via a loop or other timing methods.
4. Therefore, in simple terms, the sensor watches when the ball is being dropped. When it experiences a ball drop, it starts a timer and keeps watching for 75 microseconds, capturing the data during this time window. It is like taking a super quick snapshot of what's happening right after the drop occurs.

The sensors, including strain gauges, accelerometers, and acoustic emission sensors, were calibrated by observing the peak values under known controlled conditions. The peak sensory values were measured during a series of standardized tests to establish baseline readings, ensuring that any deviations during the experiment would accurately reflect structural changes or damages.



Fig 4. Ball Drop Setup

Ball Drop Test Setup: For the ball drop test setup, we utilized a stand with an inscribed scale, C clamps, sample plates, accelerometers, a load cell, LabView, a USB-6001 data recording device, standard weights, and a 33-gram steel ball. C clamps were used to ensure that the test material was held in position. To execute the ball drop test accurately, the ball was kept parallel to the corresponding height by referencing the scale on the stand. To obtain readings with minimal error, accelerometers were positioned on top of the plate while the load cell was situated underneath it. The test setup is shown in Figure 4.

Environmental factors, such as temperature and humidity, the experiments were conducted in a controlled laboratory environment where these variables were monitored and maintained within stable ranges. This step ensured that external environmental conditions did not interfere with sensor outputs, minimizing the risk of data skew due to factors unrelated to structural health. To simulate the conditions of an aircraft panel under impact, a metal ball was employed. This ball was dropped from a specific height and directed to strike the test material, which was securely held using clamps. The test material was presumed to represent an aircraft panel, and the impact resulting from the ball drop was observed and recorded. Table 2 shows the deflection v/s applied load for the acrylic sheet and Carbon-Glass hybrid composite.

Table 2. Deflection voltage for loads

Load (gm)	Acrylic Load cell	CGF-Load cell
0	-8.23E-04	-8.73E-04
50	-8.20E-04	-8.55E-04
200	-1.28E-03	-8.62E-04
500	-2.07E-03	-9.40E-04

3 RESULT AND DISCUSSION

Numerical analysis was conducted on the composite plate with the same dimensions. The results obtained were compared with the experimental data, Table 3 represents the comparison data.

Table 3. Equivalent Stress values of Numerical and Experimental analysis

Height	Experimental	Numerical
10cm	1.1	1.0555
20 cm	2.1	2.0310
30 cm	2.12	2.0561
40 cm	2.25	2.2109

A comparative SHM analysis was conducted between acrylic and carbon fibre composite cantilever sheets as shown in Figure 5. The experimental values were compared with the simulation results and a good agreement was found.

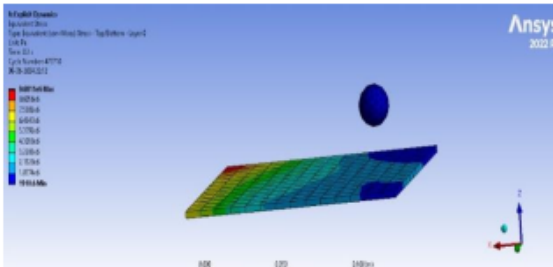


Fig. 5. Simulation Images of composite plate

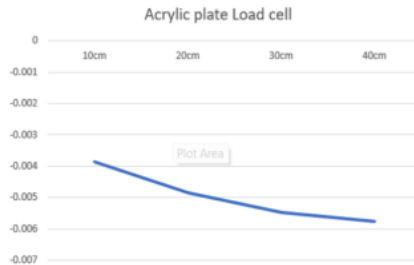


Fig. 6. Height of ball drop and Load cell output in voltage

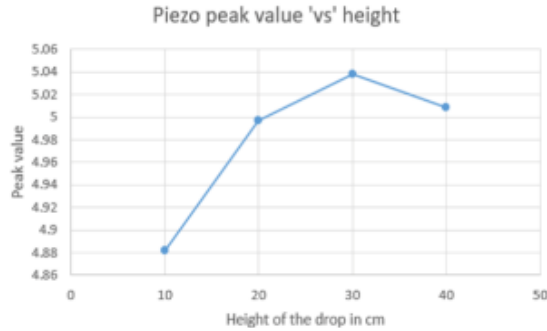


Fig. 7. Height and Voltage peak values for Acrylic Plate

The data indicate a general trend wherein the peak acceleration seems to increase with increasing ball drop height. In particular, the peak values gradually increase from 4.88187 at 10 cm to 5.03798 at 30 cm and then slightly increase to 5.00831 at 40 cm. This aligns with the expected relationship between drop height and acceleration in a gravitational field.

Cell could be a limiting factor affecting the measurements. While the values are consistently negative, there is an inconsistency in the formatting of the numbers (e.g., spaces in "- 0.00302749"). Standardizing the format would improve the clarity and consistency of the dataset. This inverse relationship with the drop height is influenced by the load cell position. All the data show a positive correlation between the height of the ball drop and the corresponding peak acceleration values. The overall trend aligns with expectations based on classical mechanics and the principle of energy conservation.

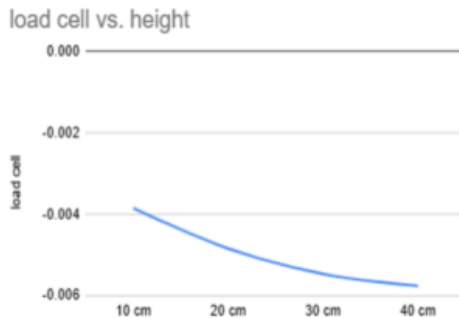


Fig. 8. Height and Voltage peak values for Composite Plate

Further analysis, considering potential limiting factors, could provide a more comprehensive understanding of the observed trends. The consistent decrease in peak values implies that the acrylic plate effectively absorbs and dissipates energy, indicating a dampening or resistant response to the impact force. This behaviour underscores the plate's ability for efficient energy absorption and dissipation in response to varying drop heights.

Table 4. Voltage Output for acrylic and CGF

Height	Piezo accelerometer		Load cell	
	Acrylic	CGF	Acrylic	CGF
10	4.2458	4.88187	-0.0038516	-0.00332597
20	4.73995	4.99669	-0.0048451	- 0.00302749
30	4.82768	5.03798	-0.0054721	-0.00333355
40	4.95541	5.00831	-0.0057638	-0.00297372

The readings increased with increasing drop height. This suggests that the impact force or pressure on the piezo sensor tends to increase as the drop height increases. The recorded measurements exhibit a consistent trend for each drop height, indicating relatively stable values. However, variations are observed between the 10 cm and 20 cm measurements, where there is a more pronounced increase from 4.2458 to 4.73995. In contrast, the discrepancies between the 30 cm and 40 cm values appear to be relatively small. This suggests that the impact on the piezo sensor is more distinguishable when it transitions from a 10 cm drop height to a 20 cm drop height than it is for subsequent increments in height. The strong agreement between experimental results and numerical predictions demonstrates the validity of our approach and highlights the promising future of sensor-based SHM for materials research. This correlation underscores the potential for significant advancements in SHM technology, suggesting a bright outlook for continued innovation in this field. The findings indicate that in cases where loads are applied due to sudden gusts or other anticipated scenarios, the SHM system can be configured to issue a warning. This capability is achieved by establishing a threshold input frequency that corresponds to the structural response under limiting conditions. If this frequency exceeds the structural limits, it signals potential damage in specific aircraft components.

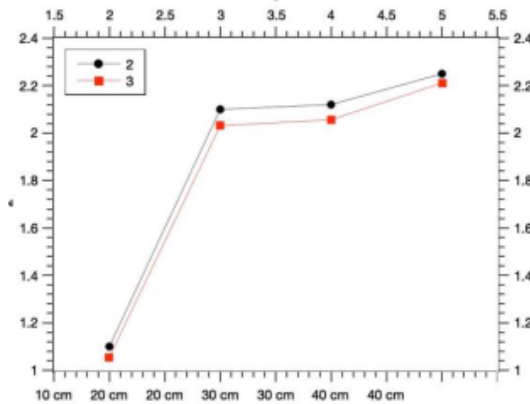


Fig. 9. Comparison of experimental and numerical analysis data

The acrylic plate demonstrated a greater capacity for absorbing and dissipating impact energy, as evidenced by the lower peak acceleration values at higher drop heights. This suggests that acrylic, due to its inherent material properties, is better suited for impact mitigation. On the other hand, the carbonglass hybrid composite displayed a higher peak acceleration, indicating a stiffer response with less energy absorption.

This can be attributed to the higher stiffness and strength of the composite material, making it less flexible but better at withstanding larger loads without permanent deformation. The study corroborates previous studies in literature that have shown the trade-offs between energy absorption and load-bearing capacity in different materials used for impact protection and structural applications [17], [18]. Furthermore, the differences in energy dissipation between the materials highlight their respective suitability for different structural applications in aerospace. The ability of the SHM system to accurately capture these variations emphasizes its critical role in material selection and damage prediction.

This analysis not only validates the experimental setup but also provides insights into how material properties influence structural behavior, aiding in the selection of appropriate materials for various aerospace components. This advanced monitoring capability significantly enhances maintenance operations, making them quicker and more efficient. By providing real-time alerts about the structural integrity of the aircraft, maintenance crews can prioritize inspections and repairs based on the severity of the warnings. Such a proactive approach not only ensures safety but also minimizes downtime, enabling timely interventions before minor issues escalate into major failures. Ultimately, the implementation of these SHM techniques contributes to a safer and more reliable aviation environment, enhancing overall operational efficiency and aircraft longevity.

4 CONCLUSION

This study demonstrates the critical role of SHM (SHM) in aerospace applications, emphasizing its potential to enhance safety, reduce maintenance costs, and extend aircraft service life. Through experimental analysis comparing acrylic and carbon-glass hybrid composite materials, we observed consistent correlations between impact forces and sensor outputs. The integration of various sensors, including piezoelectric vibration sensors, accelerometers, and load cells, provided comprehensive data on structural responses to controlled impacts. The comparison of experimental results with numerical simulations validated the effectiveness of the SHM system. This research underscores the importance of advanced SHM techniques in modern aircraft maintenance and safety management, paving the way for more reliable and efficient air transportation systems.

Acknowledgements: The authors want to acknowledge the anonymous reviewers who give useful suggestions to the manuscript. The authors also acknowledge Dr. Stanley Samlal and Mr. Samuel Vivek Williams for their guidance during the experimental process.

REFERENCES

1. M. M. Azad, S. Kim, Y. B. Cheon, and H. S. Kim, "Intelligent structural health monitoring of composite structures using machine learning, deep learning, and transfer learning: a review," *Adv. Compos. Mater.*, vol. 33, no. 2, pp. 162–188, Mar. 2024, doi: 10.1080/09243046.2023.2215474
2. "Structural health monitoring," Wikipedia. Sep. 07, 2023. Accessed: Dec. 15, 2023. [Online]. Available: https://en.wikipedia.org/w/index.php?title=Structural_health_monitoring&oldid=1174221034
3. V. Vijay Kumar, G. Balaganesan, J. K. Y. Lee, R. E. Neisiany, S. Surendran, and S. Ramakrishna, "A Review of Recent Advances in Nanoengineered Polymer Composites," *Polymers*, vol. 11, no. 4, p. 644, Apr. 2019, doi: 10.3390/polym11040644
4. V. V. Kumar, S. Rajendran, and S. Ramakrishna, "Experimental analysis of ballistic impact on carbon, glass and hybrid composite under hydrostatic prestrain," in *Advances in the Analysis and Design of Marine Structures*, CRC Press, 2023
5. X. Huang, P. Wang, S. Zhang, X. Zhao, and Y. Zhang, "Structural health monitoring and material safety with multispectral technique: A review," *J. Saf. Sci. Resil.*, vol. 3, no. 1, pp. 48–60, Mar. 2022, doi: 10.1016/j.jnlssr.2021.09.004
6. V. Giurgiutiu and C. Soutis, "Enhanced Composites Integrity Through Structural Health Monitoring," *Appl. Compos. Mater.*, vol. 19, no. 5, pp. 813–829, Oct. 2012, doi: 10.1007/s10443-011-9247-2
7. V. V. Kumar, S. Rajendran, G. Balaganesan, S. Surendran, A. Selvan, and S. Ramakrishna, "High velocity impact behavior of Hybrid composite under hydrostatic preload," *J. Compos. Mater.*, vol. 56, no. 24, pp. 3769–3779, Oct. 2022, doi:10.1177/00219983221122923
8. M. Vijayan, V. Selladurai, V. Vijay Kumar, G. Balaganesan, and K. Marimuthu, "Low Velocity Impact Response of Nano-Silica Reinforced Aluminum/PU/GFRP Laminates," in *Dynamic Behavior of Soft and Hard Materials Volume 1*, R. Velmurugan, G. Balaganesan, N. Kakur, and K. Kanny, Eds., Singapore: Springer Nature, 2024, pp. 433–442. doi: 10.1007/978-981-99-6030-9_38
9. A. D. Nugraha et al., "Investigating the mechanical properties and crashworthiness of hybrid PLA/GFRP composites fabricated using FDM-filament winding," *Heliyon*, vol.10, no. 20, p. e39062, Oct. 2024, doi: 10.1016/j.heliyon.2024.e39062
10. Y. Chen and X. Xue, "Advances in the Structural Health Monitoring of Bridges Using Piezoelectric Transducers," *Sensors*, vol. 18, no. 12, p. 4312, Dec. 2018, doi: 10.3390/s18124312
11. J. Sun, D. Chen, C. Li, and H. Yan, "Integration of scheduled structural health monitoring with airline maintenance program based on risk analysis," *Proc. Inst. Mech. Eng. Part O J. Risk Reliab.*, vol. 232, no. 1, pp. 92–104, Feb. 2018, doi: 10.1177/1748006X17742777
12. V. Giurgiutiu, "16 - Structural health monitoring (SHM) of aerospace composites," in *Polymer Composites in the Aerospace Industry*, P. E. Irving and C. Soutis, Eds., Woodhead Publishing, 2015, pp. 449–507. doi: 10.1016/B978-0-85709-523-7.00016-5
13. "What is an Arduino? - SparkFun Learn." Accessed: Sep. 28, 2024. [Online]. Available: <https://learn.sparkfun.com/tutorials/what-is-an-arduino/all>
14. "USB-6001 Specifications - NI." Accessed: Dec. 15, 2023. [Online]. Available: <https://www.ni.com/docs/en-US/bundle/usb-6001-specs/resource/374369a.pdf>
15. "Vibration Sensor Module | Sharvielectronics: Best Online Electronic Products Bangalore." Accessed: Sep. 28, 2024. [Online]. Available: <https://sharvielectronics.com/product/vibration-sensor-module/>

16. “Ceramic Analog Piezo Vibration Sensor Module,” Phipps Electronics. Accessed: Sep. 28, 2024. [Online]. Available: <https://www.phippselectronics.com/product/ceramic-analog-piezo-vibration-sensor-module/>
17. V. Vijay Kumar, S. Rajendran, S. Surendran, and S. Ramakrishna, “Enhancing the properties of Carbon fiber thermoplastic composite by nanofiber interleaving,” in 2022 IEEE International Conference on Nanoelectronics, Nanophotonics, Nanomaterials, Nanobioscience & Nanotechnology (5NANO), Apr. 2022, pp. 1– 4. doi: 10.1109/5NANO53044.2022.9828924.
18. V. Vijay kumar, S. Rajendran, S. Ramakrishna, and S. Sankunny, “Experimental investigation of carbon and glass hybrid composite under ballistic impact for marine applications,” 2022, p. 5. doi: 10.1201/9781003320272-15/experimentalinvestigation-carbon-glass-hybrid-compositeballistic-impact-marine-applications-kumarrajendran-ramakrishna-surendran.

Open Access This chapter is licensed under the terms of the Creative Commons Attribution-NonCommercial 4.0 International License (<http://creativecommons.org/licenses/by-nc/4.0/>), which permits any noncommercial use, sharing, adaptation, distribution and reproduction in any medium or format, as long as you give appropriate credit to the original author(s) and the source, provide a link to the Creative Commons license and indicate if changes were made.

The images or other third party material in this chapter are included in the chapter's Creative Commons license, unless indicated otherwise in a credit line to the material. If material is not included in the chapter's Creative Commons license and your intended use is not permitted by statutory regulation or exceeds the permitted use, you will need to obtain permission directly from the copyright holder.

